catalysts

MDPI

Article

Stable Sulfonic MCM-41 Catalyst for Furfural Production from Renewable Resources in a Biphasic System

Yasnina Olivares [1,2], Carla Herrera [1,2], Juan Seguel [1,2], Catherine Sepúlveda [1,2], Carolina Parra [2,3,*] and Gina Pecchi [1,2,*]

[1] Facultad de Ciencias Químicas, Universidad de Concepción, Edmundo Larenas 129, Concepción 4070409, Chile
[2] Millennium Nucleus on Catalytic Processes towards Sustainable Chemistry (CSC), Santiago 2530388, Chile
[3] Centro de Biotecnología, Universidad de Concepción, Concepción 4070409, Chile
* Correspondence: roparra@udec.cl (C.P.); gpecchi@udec.cl (G.P.)

Abstract: An MCM-41-SO_3H catalyst with 14 wt% S was successfully synthesized to be used in furfural production from xylose and hemicellulose in a biphasic n-butanol/water system. The precursor MCM-41 and the acid-functionalized MCM-41-SO_3H catalyst were characterized by XRD, FTIR, TEM, N_2 physisorption, ICP-MS, TPD-NH_3, and XPS. The characterization results indicated that the sulfonic process partially decreased the ordered mesoporous structure and increased the acid strength of the initial MCM-41. The catalytic performance of the xylose conversion was evaluated in a batch-type reactor using different biphasic ecological and renewable n-butanol/water ratios (1:1, 1.5:1, 2:1, and 2.5:1) as dissolvent at 170 °C. The effect of the dissolvent mixture was clearly seen from the larger initial reaction rate and TOF values for the 1.5:1 ratio. This catalytic behavior indicated that a proper proportion of n-butanol/water dissolvent mixture enhanced the solubility of the substrate in the n-butanol-rich mixture and prevented the deactivation of acidic sulfonated surface groups. To achieve transformation of lignocellulosic raw material to value-added products, the MCM-41-SO_3H catalyst was also used for the production of furfural. The recycling evaluation tests indicated that for the recovered catalyst submitted to a sulfonation process, the yield of furfural was closer to the fresh catalyst.

Keywords: MCM-41-SO_3H; xylose; hemicellulose; furfural; biphasic

Citation: Olivares, Y.; Herrera, C.; Seguel, J.; Sepúlveda, C.; Parra, C.; Pecchi, G. Stable Sulfonic MCM-41 Catalyst for Furfural Production from Renewable Resources in a Biphasic System. *Catalysts* **2023**, *13*, 1024. https://doi.org/10.3390/catal13061024

Academic Editors: Ileana Daniela Lick, Paula Osorio-Vargas and Ivan V. Kozhevnikov

Received: 25 January 2023
Revised: 13 June 2023
Accepted: 14 June 2023
Published: 20 June 2023

1. Introduction

The use of low-cost raw materials with low environmental impact, such as urban, forest, or agricultural waste of lignocellulosic origin, to obtain clean energy or bioenergy as well as platform molecules or building blocks is still a challenge. Lignocellulosic biomass is composed of a mixture of cellulose, lignin, and hemicellulose connected through chemical bonds [1]. These biomass fractions can be promising raw materials for energy generation and/or biomaterials [2]. Hemicellulose is the second most abundant polysaccharide in plant cell walls, accounting for 15 to 30% of lignocellulosic biomass by weight [3]. Due to its nature and physicochemical properties, it is a suitable raw material to produce a wide variety of new materials and chemicals with added value [4]. Via catalytic transformation furfural [5], a selective solvent can be obtained from xylose, which is present as xylan in hemicellulose, for the refining of lubricating oils and diesel fuels, plastics, and agrochemical products. Furfural has been identified as one of the top 10 biomass-derived chemicals [6]. In the commercial sector, the furfural process is operated with a high toxicity and corrosive homogeneous H_2SO_4 catalyst under batch and continuous conditions. The replacement of this hazardous homogeneous catalyst with environmentally compatible and reusable heterogeneous catalysts has been one of the key areas of green chemistry [7,8].

MCM-41 is a well-known ordered mesoporous silica material that is widely used as a heterogeneous catalyst in various chemical reactions, primarily due to its hexagonal arrangement of uniformly sized one-dimensional pores and its reliable synthesis. It possesses a pore diameter ranging from 2 to 10 nm and mesoporous volume ranging from 0.7 to 1.2 $cm^3\ g^{-1}$ and has a large, easily accessible internal area [7,9–12]. To increase the acid strength of MCM-41 and its applications in heterogeneous catalysis, separation processes, and nanoengineering, pure silica MCM-41 can be functionalized with SO_3-H groups [13] or partially replaced by a heteroatom (Ti-doped) [6]. The presence of sulfonic groups increases the acid strength of MCM-41 [14,15]. Due to their several advantages, such as reusability, environmental compatibility, non-corrosiveness, and easy separation, the sulfonated ordered mesoporous silica MCM-41-SO_3H has been largely used as a heterogeneous catalyst in dehydration reactions. The selective catalytic dehydration reaction of xylose to furfural using sulfonated ordered mesoporous silica with a tunable pore structure and tailored composition has gained much research interest [8]. For the selective catalytic dehydration reaction of xylose and xylan to furfural, Dias et al. [16] reported 81% conversion and 47% selectivity to furfural at a reaction temperature of 140 °C using DMSO/water as dissolvent in 4 h. On the other hand, Zang et al. [17] reported 90% conversion and 40% selectivity to furfural at a reaction temperature of 170 °C using MCM-41 and butanol/water as biphasic dissolvent. In comparison, with a homogenous acid H_2SO_4 reaction medium, Shi et al. [15] reported a yield of 63% of furfural from xylan in 4 h at 160 °C.

It has been recognized that furfural has great commercial added value as the starting molecule for many other products of industrial interest and also as an intermediate product in the manufacture of solvents such as tetrahydrofuran (THF); methyl tetrahydrofuran (MeTHF); furfuryl alcohol; and succinic, maleic, and levulinic acids. This condition makes furfural one of the highest value-added chemical products derived from biomass [18]. To improve the furfural yield in a green way, catalytic reactions have been carried out using different solvents, such as dimethyl sulfoxide (DMSO) [16], toluene [19], 1-butanol [17], and ionic liquids [20,21]. For the use of biphasic aqueous systems as dissolvent, an immiscible mixture of water and an organic solvent can be more efficient as reaction medium because the products produced in the aqueous phase and soluble products produced in the organic phase can be easily extracted and separated from the organic phase.

In this study, a functionalized MCM-41-SO_3H silica was synthetized according to the method described by Marin-Astorga et al. [22] and Rostamizadeh et al. [23] to be used in the selective dehydration reaction of xylose and hemicellulose to furfural in a biphasic butanol/water mixture. The influence of the dissolvent mixture (different butanol/water ratios of 1:1, 1.5:1, 2:1, and 2.5:1) on the catalyst activity and selectivity for furfural production was assessed. A full characterization of the MCM-41-SO_3H catalyst was also conducted. Furthermore, to determine industrial application, the MCM-41-SO_3H catalyst was evaluated for selective hemicellulose dehydration to furfural. Considering the environmental requirements, recyclability tests were performed to evaluate the catalyst's stability, selectivity, and catalytic performance.

2. Results and Discussion

2.1. ICP

To evaluate the reproducibility of the –SO_3H functionalization, the sulfonation process was carried out twice. As shown in Table 1, synthesis was achieved with a content of 15 wt% S in the MCM-41-SO_3H catalyst. The same H, N, and C contents of 5%, <2%, and <0.1%, respectively, were observed for both MCM-41-SO_3H-1 and MCM-41-SO_3H-2.

2.2. N_2 Physisorption

The N_2 adsorption–desorption isotherms of MCM-41 and the MCM-41-SO_3H catalyst are shown in Figure 1. Both materials displayed type IV isotherms characteristic of ordered mesoporous materials of uniform pore size with a H1 hysteresis indicating a narrow distribution of pores [9]. The lowest amount of nitrogen adsorbed for the MCM-41-SO_3H

catalyst indicated loss of the mesoporous structure after the sulfonating process. As shown in Table 1, the textural characterization properties showed a significant decrease in the specific surface area (SBET) with the sulfonating process. This was attributed to the pore surface being covered by the sulfonic groups. These S_{BET} values are also in line with Dias et al. [16], who reported values of 833 m^2g^{-1} for MCM-41 and 400 m^2g^{-1} for MCM-41-SO_3H. To remove the surface covering by the sulfonic groups, Khan et al. [24] used a previous degassing treatment at 150 °C for 10 h under nitrogen flow and reported an estimated pore size of 2.5 nm and a surface area of 889 m^2 g^{-1} for MCM-41 and a reduction in pore size to 2.2 nm and a surface area of 805 m^2 g^{-1} for MCM-41-SO_3H. The surface values for MCM-41-SO_3H were lower due to the pores being covered by the sulfonic groups, which obstructed the passage of N_2 molecules. In addition, a decrease in the specific surface area (SBET) due to nonstructural porosity consisting of some irregular cavities that permeate the entire bulk and give rise to a secondary porosity [25] cannot be ruled out.

Table 1. Elemental analysis, specific surface area, and acid distribution for the synthesis of the MCM-41 precursor and the MCM-41-SO_3H-1 and MCM-41-SO_3H-2 catalysts.

	% S	% H	% N	%C	S_{BET}, m^2g^{-1}	Acid Sites (mmol g^{-1})		
						Weak	Medium	Total
MCM41-1	<0.1	<2	<2	<0.1	1025	-	-	-
MCM41-SO_3H-1	14.6	5.3	<2	<0.1	243	1.4	0.9	2.3
MCM41-SO_3H-2	14.1	5.2	<2	<0.1	256	1.7	1.0	2.7

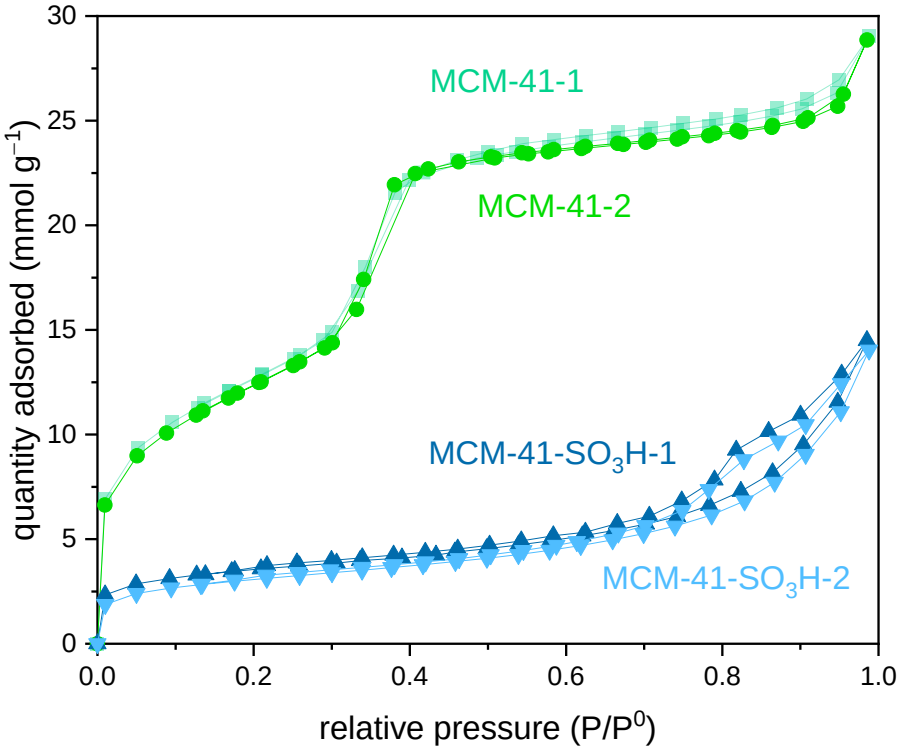

Figure 1. N_2 adsorption isotherms of MCM-41 and the MCM-41-SO_3H catalyst.

2.3. TPD-NH_3

Figure 2 displays the temperature-programmed desorption (TPD) of NH_3 patterns of the MCM-41-SO_3H-1 and MCM-41-SO_3H-2 catalysts. To better demonstrate the sulfonation process, the patterns of MCM-41 are also included in the figure. As can be seen, there were large desorption peaks for the two sulfonated catalysts with almost the same desorption

profile, indicating the reproducibility of the sulfonating process. No desorption peaks were detected for MCM-41, while large and well-defined peaks were observed for weak and medium to large acid sites for MCM-41-SO_3H-1 and MCM-41-SO_3H-2 catalysts. The differences between MCM-41 and the MCM-41-SO_3H catalysts were attributed to acid sites generated from the –SO_3H groups, indicating a higher total number of acid sites than the initial MCM-41. This can be also seen in Table 1, which shows the total number of acid sites connected to the decomposition of the SO_3H group compared to MCM-41. Hermida et al. [26] reported the absence of acid sites in SBA-15 for the HSO_3SBA-15 catalyst, confirming that it is a neutral material. For HSO_3SBA-15, the propyl sulfonic groups appeared as two peaks corresponding to weak and medium acid sites that began to decompose at higher temperatures (427–527 °C). This result is in accordance with that previously demonstrated by Sreevardhan et al. [27] for a similar mesoporous catalyst. For the SBA-15-SO_3H material, the authors reported a desorption signal centered on a Tmax of 600 °C and another small and intense signal centered on a Tmax of 380 °C, which led them to conclude that there was decomposition/desorption of the SO_3H groups, indicating that SBA-15-SO_3H is thermally stable up to 350 °C. The total number of acid sites determined by temperature-programmed desorption of ammonia was much higher in the case of the catalyst SBA-15-SO_3H (0.125 mmol g cat^{-1}) compared to SBA-15 (0.013 mmol g cat^{-1}) [27].

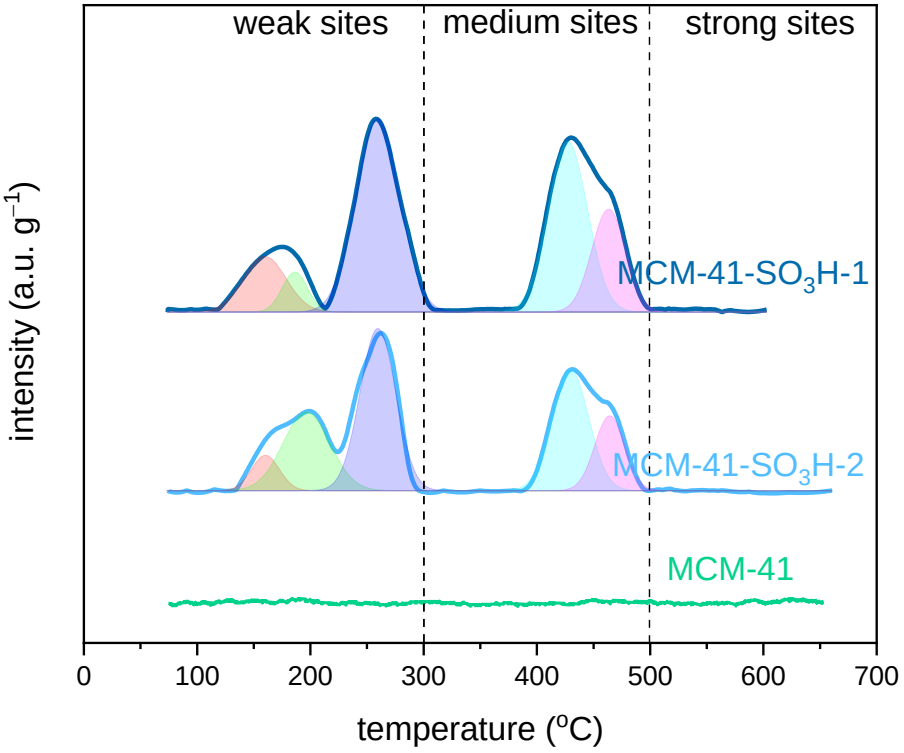

Figure 2. NH_3 DTP profiles of MCM-41 and the MCM-41-SO_3H-1 and MCM-41-SO_3H-2 catalysts.

2.4. XRD

The low-angle X-ray diffraction patterns of MCM-41 and the MCM-41-SO_3H catalyst are shown in Figure 3. For MCM-41, the expected planes at 2θ = 2.04, 3.63, 4.23, and 5.59 corresponding to the Miller index (100), (110), (200), and (210) were clearly detected. For the MCM-41-SO_3H catalyst, a slight decrease in the intensities was seen with the first three Bragg peaks maintained, indicating that the hexagonal symmetry of the mesoporous material was preserved. This result is in line with those obtained by other researchers with a similar XRD pattern of MCM-41-SO_3H [8,16]. On the other hand, Dias et a [16] attributed the attenuation of the XRD peaks to a reduction in the X-ray scattering contrast between the silica walls and the sulfonic groups present in the pores and not to a loss of structural order.

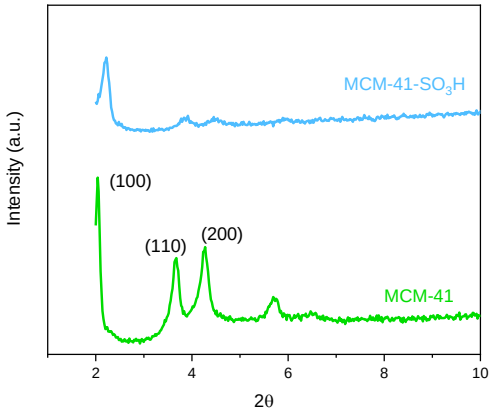

Figure 3. Diffraction patterns of MCM-41 and the MCM-41-SO_3H catalyst.

2.5. TEM

Figure 4 shows the TEM micrographs of MCM-41 and the MCM-41-SO_3H catalyst. For MCM-41, well-defined hexagonal structures were seen. After the sulfonation process, some amorphous agglomerates with partial loss of the hexagonal arrangement corresponding to the MCM-41 structure was observed [11]. The presence of areas with hexagonal pores in the MCM-41-SO_3H catalyst indicated that partial loss of the mesoporous structure occurred when the mesoporous material MCM-41 was sulfonated. This result is in agreement with XRD results and a previous study by Sarrafi et al. [8], who reported that the mesoporous structure of the MCM-41 material remained with the addition of sulfonic groups.

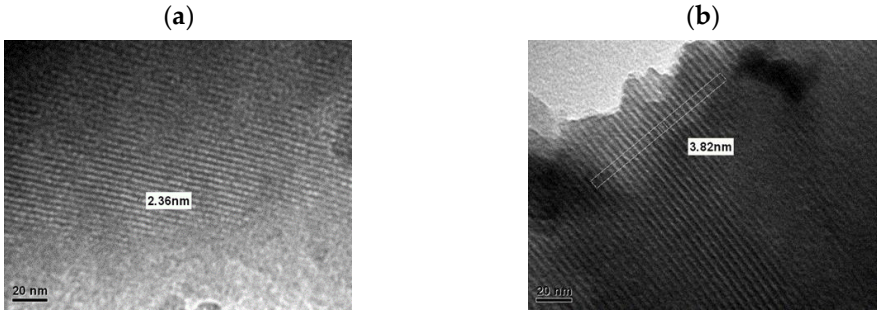

Figure 4. TEM micrographs: (**a**) MCM-41, (**b**) MCM-41-SO_3H catalyst.

2.6. FTIR

The presence of the sulfonic groups on the MCM-41-SO_3H catalyst was also confirmed by FTIR spectra. The FTIR spectra of the materials are shown in Figure 5. The infrared spectrum showed characteristic peaks of mesoporous silica attributed to the asymmetric stretching of the O–H bond located at 3392 cm^{-1} [28], asymmetric vibrations of Si–O–Si at 1066 cm^{-1} [29], symmetrical stretching of the Si–O bond at 807 cm^{-1}, and Si–O–Si bond splitting at 463 cm^{-1} [30]. In the same figure, it is possible to observe two peaks at 2850 and 800 cm^{-1}, which corresponded to signals of the Si–C and C–H bonds, characteristic of the MCM-41 types of mesoporous materials 24. Regarding the sulfonation process (Figure 5), the band observed at 1165 cm^{-1} corresponded to the stretching of the S=O bond [16,28] and confirmed the presence of the sulfonic group on the MCM-41-SO_3H catalyst. The bands identified for the synthesized sulfonated material corresponded to those previously reported by Sheng et al. [28] for this type of material, with the sulfonic group corresponding to the stretching of the S=O bond at 1169 cm^{-1} and S–O at 574 cm^{-1}. On the other hand, the authors of [29] confirmed the presence of the sulfonic group by peaks attributed to the stretching of the S–H bond at 2500 cm^{-1} and the S=O bond at 1180 cm^{-1}.

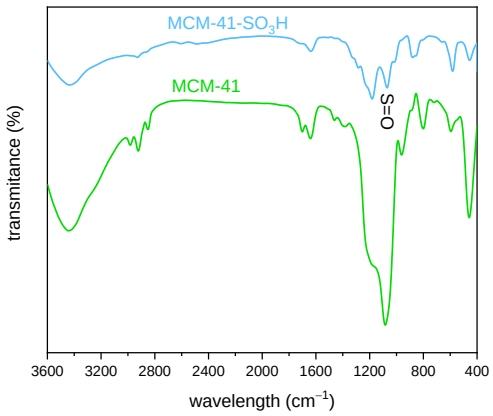

Figure 5. FTIR spectra of MCM-41 and the MCM-41-SO_3H catalyst.

2.7. XPS

The XP spectra of the Si 2p, O 1s, and S 2p are shown in Figure 6, while the binding energies (BE) are shown in Table 2. The curve fitting of the Si core-level spectrum was performed by the 2p level for MCM-41 located at 103.7 eV. For MCM-41-SO_3H, the signal was deconvoluted with a slight contribution at large BE, indicating a more polarized Si species. For MCM-41, only one type of oxygen was detected at 533.1 eV, which was attributed to O1s of Si–O–Si linkages [31]. After the sulfonation process, the curve was deconvoluted in two peaks, with the larger peak shifted 0.3 eV towards lower BE and a new contribution at 534.3 eV attributed to the sulfonic group (SO_3H). With regard to sulfur surface species, the S 2p signal at 167.4 eV was attributed to surface species of sulfonic acid (SO_3H) [32,33], while a second signal at 169.0 eV was attributed to the presence of surface S^{6+} in the SO_4^{2-} group [34], confirming the presence of surface sulfonic species. The decrease in the atomic Si/O surface ratio, as shown in Table 2, was an expected result considering the lower amount of surface Si after the sulfonating process.

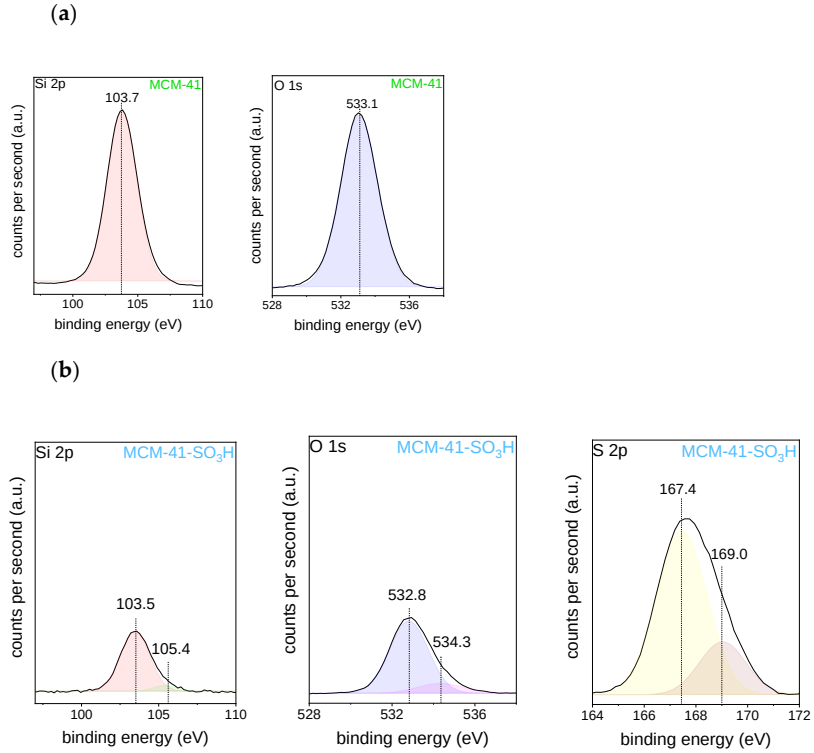

Figure 6. XPS spectra: (**a**) Si 2p and O1s of MCM-41, (**b**) Si 2p, O 1s and S 2p of MCM-41-SO_3H catalyst.

Table 2. Binding energies (eV) of core levels and atomic surface ratio of the MCM-41 precursor and the MCM-41-SO_3H catalyst.

	Binding Energy (BE), eV						Si/O	
	Si 2p		O 1s		S 2p		Si/O	Si/S
MCM-41	103.7(100) 100%	-	533.1 100%	-	-	-	0.18	-
MCM-41-SO_3H	103.5 93%	105.4 7%	532.9 88%	534.3 12%	167.4 84%	169.0 16%	0.14	1.50

2.8. Xylose Conversion

The catalytic performance of the MCM-41-SO_3H catalyst was carried out at different butanol/water ratios (1:1, 1.5:1, 2:1, and 2.5:1). For the xylose conversion, as shown in Figure 7a, there was clear effect of the nature of the dissolvent mixture on the total conversion after 4 h of reaction. It was observed that xylose conversion in equal proportion of solvents (1:1 ratio) reached 85% after 1 h of reaction. Furthermore, it was observed that xylose conversion increased with the addition of n-butanol (1.5:1 ratio) until it reached a maximum (93%). However, a further increase in the amount of n-butanol in the reaction media (2.1:1 and 2.5:1 ratios) led to a clear decrease in xylose conversion. This result suggests that a consecutive increase in the amount of n-butanol could create a hydrophobic film over sulfonic-functional groups, inhibiting their dehydration capability and thus decreasing the xylose conversion. In addition, based on the octanol–water partition coefficient, log P, xylose is more soluble in water than in n-butanol [35]. Therefore, this result points to the fact that a proper proportion of n-butanol/water dissolvent mixture is needed to enhance the solubility of the substrate in the n-butanol-rich mixture and to avoid the deactivation of acidic sulfonated surface groups. Considering the total conversion of the noncatalytic reaction was 68% at 4 h under the reaction conditions, the catalytic effect of the MCM-41-SO_3H catalyst was clearly detected [16]. Regarding the yield of furfural, as shown in Figure 7b, no large effect of the butanol/water ratio was detected, and a similar trend of xylose conversion was observed. It was observed that the catalytic yield of furfural at butanol/water ratio of 1.5:1 mixture solvent was six times higher than the noncatalytic reaction (Figure S1). Additionally, considering the catalytic reaction using MCM-41 as catalyst produced the same furfural yield as the noncatalytic reaction under the reaction condition, the large formation of furfural using the MCM-41-SO_3H catalyst was obvious [16].

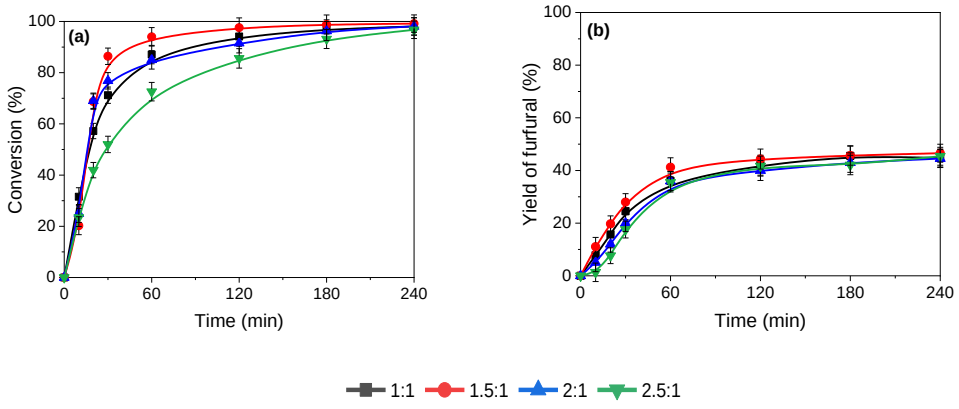

Figure 7. (**a**) Xylose conversion and (**b**) yield of furfural upon time at 170 °C and 10 bar of nitrogen for MCM-41-SO_3H catalyst at different butanol/water ratios.

The initial reaction rate (Figure 8a) and TOF values shown in Table 3 indicate a clear dependence with the butanol/water mixture ratio. The highest initial rate and TOF values were obtained for butanol/water ratio of 1.5:1. The increase in the TOF values indicated

that significantly more xylose molecules were converted over the active sites present over the MCM-41-SO_3H catalyst at butanol/water ratio of 1.5:1. It is believed that water content in the reaction medium could have negative consequences on the catalytic activity. As a result, it has been reported that there is 50% conversion and 25% selectivity to furfural in the absence of solvents [16] compared to an 8% xylose conversion at 24 h when the reaction is carried out in water.

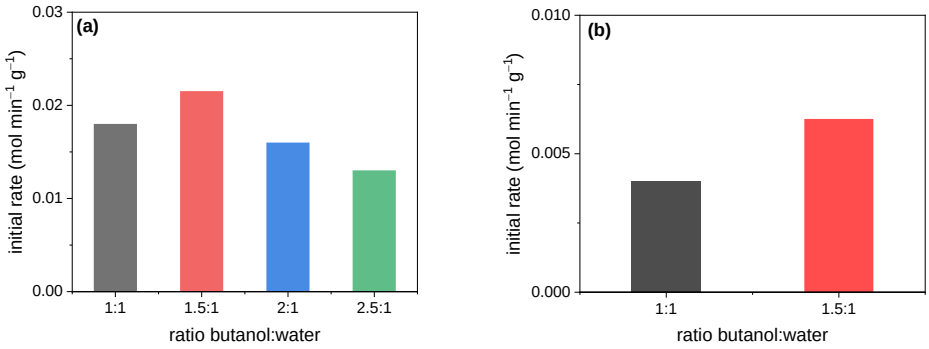

Figure 8. Initial reaction rate for MCM-41-SO_3H catalyst at different butanol/water ratios for (**a**) xylose and (**b**) hemicellulose.

Table 3. Conversion, yield of furfural, initial reaction rate, pseudo-first-order constant and TOF for xylose conversion on the MCM-41-SO_3H catalyst.

Butanol/Water Ratio	X_{TOTAL} % 2 h	Y_{FUR} % 2 h	k $h^{-1}g_{cat}{}^{-1}$	TOF s^{-1}
1:1	97	42	2.6	0.12
1.5:1	100	46	3.1	0.15
2:1	92	41	2.7	0.11
2.5:1	85	42	1.9	0.09

Reaction conditions: batch reactor, 170 °C, 700 rpm, 10 bar N_2.

Our results suggest that the nature of the organic solvent plays an important role in the conversion and selectivity results. Furthermore, when methylisobutylketone was used as the cosolvent, lower selectivity (55%) to furfural was obtained with 32% yield. This is despite the better affinity of furfural for methylisobutylketone than for toluene with 40% conversion and 85% selectivity corresponding to 34% yield [36]. It is also worth noting that Rivalier et al. reported a large selectivity to furfural in the dehydration of fructose in a solvent mixture consisting of water and toluene [37]. Aqueous solution of butanol is a very attractive substrate from an industrial point of view. When comparing the yields of furfural produced from xylose, high yields were achieved using homogeneous catalysis with mineral acids (Table S1). The yields decreased when heterogeneous catalysis was used. However, it is necessary to consider the advantages from an environmental point of view and the possibility of reusing the catalyst, among others factors.

The successful fit of the experimental data to a pseudo-first-order reaction is shown in Figure 9, allowing the global pseudo-first-order constant to be calculated. Table 3 shows the initial reaction rate and TOF values, and it can be seen that they followed the same trend as the global pseudo-first-order constant. The 46% yield of furfural for the butanol/water ratio of 1.5:1 as solvent showed that this was the proper proportion of n-butanol/water mixture needed to enhance the solubility of the substrate favoring the required number of acid sites in the MCM-41-SO_3H catalyst. Additionally, the regular and well-ordered hexagonal array provided nanosized microreactors that favored the accessibility of the reactant [23,38].

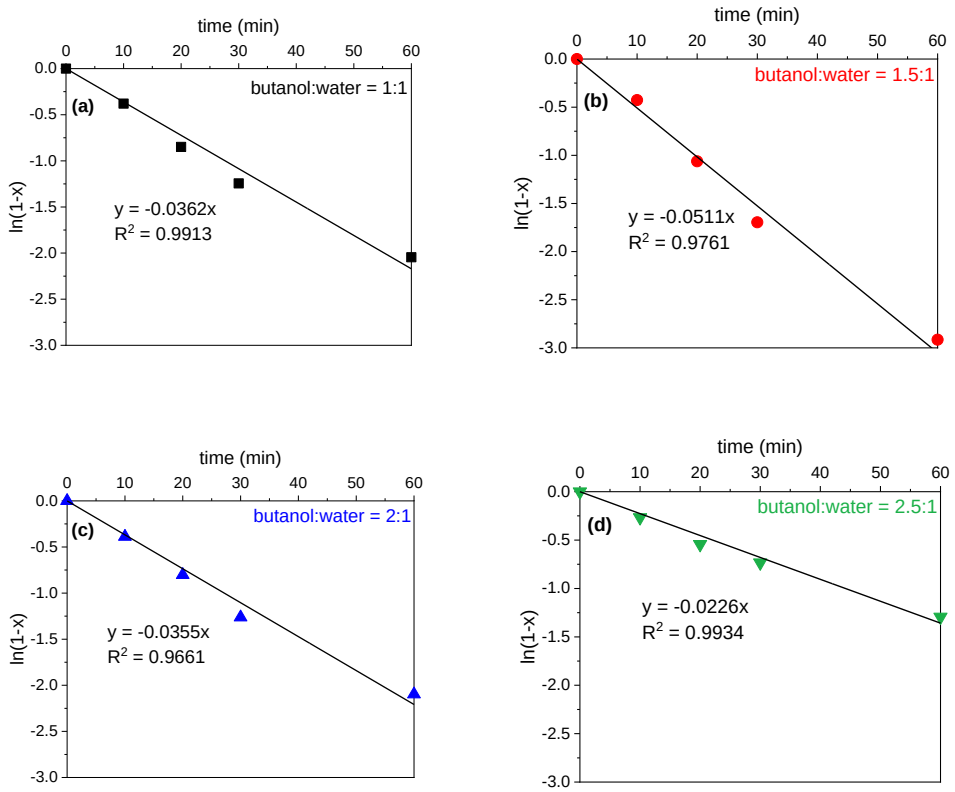

Figure 9. (**a**–**d**) Pseudo-first-order adjustment for the MCM-41-SO_3H catalyst.

2.9. Hemicellulose Conversion

To go one step further in using raw materials as substrate, for the two best butanol/water ratios, the catalytic performance of the MCM-41-SO_3H catalyst was evaluated in the hemicellulose conversion, as shown in Figure 10a. As can be observed, there was a large conversion of hemicellulose reaching almost 100% of conversion at 30 min of reaction for both butanol/water ratios. This result was almost the same as that for the noncatalytic or the MCM-41 catalytic hemicellulose conversion. Therefore, to point out the enhancement of the catalytic performance of the MCM-41-SO_3H catalyst, it is important to discuss the yield of furfural. In Figure 10b, it can be observed that the catalytic conversion of hemicellulose on the MCM-41-SO_3H catalyst produced 36% furfural at both butanol/water ratios. This is a noteworthy result as the noncatalytic and MCM-41 catalytic hemicellulose conversion reactions did not produce furfural (results not shown). This behavior was previously reported by Liu et al. [39], who noted that the mechanism of the conversion of xylan to furfural in the presence of Lewis and Brønsted type acid catalysts proceeds through a reaction via depolymerization–isomerization–dehydration and that the more complex the substrate, the more the acid strength required. From Table S1, it is possible to compare the other systems that were assessed for furfural production from hemicellulose based on a mixture of solvents with up to 50% yield. However, the disadvantages that these entail have been widely discussed in the literature [21]. Therefore, the furfural production in the MCM-41-SO_3H catalyst deals with the acidity of the catalyst. Regarding the initial reaction rate (Figure 8b), lower values compared to the xylose conversion were obtained and showed the same trend, i.e., the highest initial rate was obtained for butanol/water ratio of 1.5:1.

2.10. Catalyst Recycling

The reusability of the MCM-41-SO_3H catalyst was investigated in the xylose and hemicellulose conversion. The procedure consisted of carrying out four consecutive cycles under the same reaction conditions to recover the catalyst by filtration. After each reaction

cycle, the recovered catalyst by filtration from the reaction medium was washed with a mixture of methanol with water and dried in an oven at 50 °C for 6 h. To study the effect of the recovered catalyst pretreatment, a fraction of the recovered catalyst was subjected to a new sulfonation process, and its catalytic activity was subsequently evaluated. It was found that the conversion of xylose and hemicellulose with the recycled nonsulfonated and recovered sulfonated catalysts did not show significant differences compared to the fresh catalyst. Due to the 170 °C temperature, both substrates were converted (Figure S2). Figure 11 shows the yield of furfural over time for the sulfonated and nonsulfonated recovered catalysts. To make a better comparison, the values for the fresh catalyst are also shown. The nonsulfonated catalysts displayed a negligible yield of furfural in the conversion of xylose and did not produce furfural in the hemicellulose conversion. Dias et al. observed a similar phenomenon when studying the same catalyst with toluene in the solvent mixture and at 140 °C. They attributed the loss of selectivity to the accumulation of reaction by-products on the catalyst surface [16]. A similar effect was reported by Jeong et al. in aqueous solution at 170 °C [14]. The low hydrothermal stability of MCM-41 and the effect this could have on the leaching of –SO_3H acid groups is also mentioned in the literature [14,40]. In our case, this can be explained by the loss of approximately 70% of the –SO_3H acid groups during the reaction. The amount of sulfur in the catalyst was 14% and decreased to 4.5% at the end of the reaction. Meanwhile when the recovered catalyst was submitted to a sulfonation process, the production of furfural for both substrates was recovered to values slightly lower than the fresh catalysts. This behavior indicates leaching of the active –SO_3H groups, which can be recovered with a new sulfonation process. One of the challenges that remains evident is to find a way to strengthen the union between MCM-41 and the SO_3H acid groups to stabilize the catalyst.

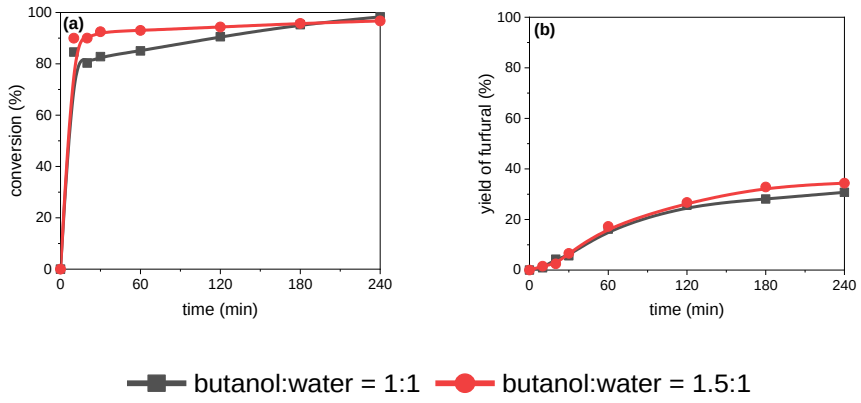

Figure 10. (**a**) Hemicellulose conversion and (**b**) yield of furfural over time at 170 °C and 10 bar of nitrogen for the MCM-41-SO_3H catalyst at different butanol/water ratios.

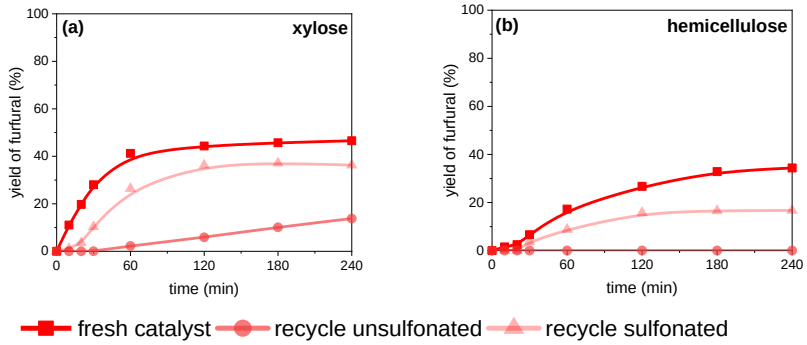

Figure 11. Yield of furfural over time of the fresh and recycled MCM-41-SO_3H catalyst at butanol/water ratio of 1.5:1 for (**a**) xylose and (**b**) hemicellulose.

A hot filtration experiment was carried out to verify what was detected regarding catalyst leaching during the catalytic conversion of xylose to furfural. According to the results obtained (Figure 11a), 30 min was considered as the half-reaction time. The reaction was stopped after 30 min, filtered while hot, and continued without the presence of the catalyst. The yield of furfural reached in the first 30 min corresponded to 27%. The yield at the final time of the reaction was 32.5% (Figure S3), which showed that part of the catalyst was affected by leaching during the course of the reaction.

3. Materials and Methods

3.1. Synthesis of the Catalyst

The MCM-41 was synthesis by the reaction of tetramethylammonium hydroxide (TMAOH) and cetyltrimethylammonium bromide (CTMABr) with aerosil silica with continuous stirring as in the standard procedure [22]. The resulting homogeneous gel had a composition of SiO_2:0.15CTMABr:0.26TMAOH:24.3 H_2O and was dried and calcined for 1 h in flowing N_2, followed by 12 h in a dynamic air flux at 500 °C for both calcinations. The –SO_3H functionalization was carried out post-synthetically according to the literature report [23]. Chlorosulfonic acid was used as functionalization reagent, which was added drop by drop by means of a funnel to a flask containing the MCM-41 under constant agitation for 30 min. The reaction was raised in an extraction bell, and the HCl (g) was released by a gas output tube.

3.2. Characterization Techniques

X-ray diffraction (XRD) was performed on a Rigaku X-ray Geigerflex using a Ni filter and Cu Kα radiation at 2–90° in 2θ range. Fourier transform infrared spectra (FTIR) was recorded in a Nicolet Magna-IR 550 instrument equipped with a quartz sample holder with KBr windows using a sample/KBr ratio of 1:150. The mesoporous structure was observed in TEM micrographs obtained in a JEOL Model JEM-1200 EX II instrument. N_2 adsorption–desorption isotherms were recorded at −196 °C in an ASAP 2010 Micromeritics apparatus, and the specific surface areas were determined by the BET equation. The chemical analysis was performed by inductively coupled plasma mass spectrometry on a PerkinElmer Elas 6000ICP-MS spectrometer. The acidity of the solid materials was determined by temperature-programmed desorption of ammonia (TPD-NH_3) using a Micromeritics 3Flex equipment. The sample was first dried under N_2 flow at 350 °C for 30 min and cooled to 100 °C under He flow for 1 min. The sample was then saturated with 30 mL min^{-1} of NH_3 flow at 100 °C for 15 min. After saturation, the sample was cooled to ambient temperature, and TPD-NH_3 was performed at a heating rate of 10 °C min^{-1} up to 800 C in flowing He. X-ray photoelectron spectra (XPS) were recorded using an Escalab 200R spectrometer provided with a hemispherical analyzer operated in a constant pass energy mode and Mg Kα X-ray radiation (hν = 1253.6 eV) operated at 10 mA and 12 kV. Charging effects of samples were corrected by fixing the binding energy (BE) of the C1s core-level of adventitious carbon at 284.8 eV (accuracy = ±0.1 eV).

3.3. Catalytic Activity Measurements

The catalytic assays of the xylose conversion were carried out in a stainless steel (100 mL) Parr-type semibatch reactor with 0.6 g of substrate (hemicellulose or xylose), 0.3 g of MCM-41-SO_3H catalyst (MCM-41 was also evaluated) using 60 mL of a biphasic ecological and renewable n-butanol/water mixture of different ratios (1:1, 1.5:1, 2:1 and 2.5:1) as solvent. In each experiment, the substrate concentration was kept equal to 0.01 g/mL. These experimental conditions were chosen from a previous work carried out by Zhang et al. [17] for MCM-41 and 1-butanol in water as reaction medium. The reaction temperature of 170 °C under 10 bar of N_2 pressure was used with stirring at 700 rpm to avoid diffusion control. The catalytic runs conducted under negligible mass transfer resistance [41] were repeated three times for each experiment. The pseudo-kinetic constants (k) were calculated using a pseudo-first-order kinetic model for a batch reactor under similar conditions [26]. The xylose and

xylose from hemicellulose concentrations were determined by HPLC (Merck Hitachi, Hitachi High-Technology Corpotation, Tokio, Japan) equipped with a refractive index detector and an Aminex HPX-87H column (Bio-Rad, Hercules, CA, USA) at 45 °C, eluted at 0.6 mL/min with 5 mM H_2SO_4. To determine the hemicellulose concentration, a solution with 5 g/L of wheat straw hemicellulose, it was subjected to hydrolysis with 3% H_2SO_4 for 30 min at 120 °C in an autoclave. The obtained sample was analyzed by HPLC to determine the xylose content in the initial sample. To convert the concentration of monomeric xylose to xylan, the factor 0.88 was used, calculated based on the water molecules gained during the hydration of the xylans [42]. Furfural was analyzed by gas chromatography (GC-FID) and mass spectrometry using a GC–MS instrument (Shimadzu GCMS-QP5050) with helium as the carrier gas. The recycling assays were performed by filtering the catalyst from the reaction medium. The filtered catalyst was washed three times consecutively with ethanol (50 mL × 3) to clean the surface and was then dried at 100 °C for 24 h. The conversion was calculated using Equation (1), and selectivity conversion was obtained according to Equation (2):

$$X(\%) = ([(x)\text{xylose}]_0 - [(x)\text{xylose}]_t)/([(x)\text{xylose}]_0) \cdot 100 \quad (1)$$

$$Y_{FUR}(\%) = [(x)\text{FUR}]_t(\text{molL}^{-1})/([(x)\text{FUR}] + [\text{Intermediates}(x)]_t) + [\text{by products}(x)]_t)) \cdot 100 \quad (2)$$

where $[(x)\text{xylose}]_0$ is the initial concentration of xylose, and $[(x)\text{xylose}]_t$ is the concentration at different times. $[(x)\text{FUR}]_t$ corresponds to the furfural production, and $[\text{Intermediates}(x)]_t$ and $[\text{by-products}(x)]_t$ are the concentrations of intermediaries and by-products during the conversion reaction, respectively.

The initial reaction rate of the total xylose conversion was calculated from the initial slope of the xylose conversion as a function of time graphic according to Equation (3):

$$r_o = (b * n)/m \quad (3)$$

where r_o is the initial reaction rate (mol $gcat^{-1}$ min^{-1}), b is the initial slope of the xylose conversion vs time, n is the initial moles of xylose, and m the weight mass of the catalyst. Additionally, to better determine the catalytic behavior, the initial rate was normalized by the number of acid sites (mol g^{-1}) to calculate the turnover frequency (TOF, h^{-1}) according to Equation (4):

$$\text{TOF} = r_o/\text{total number of acid sites} \quad (4)$$

The average number of acid sites for the MCM-41-SO_3H catalyst was 2.5 mmol/g_{cat} for the conversion of 0.6 g of xylose, whereas the molar ratio substrate/acid site was 5.3 (molar).

4. Conclusions

This study investigated catalytic furfural production from the renewable resources xylose and hemicellulose in a batch-type reactor using an MCM-41-SO_3H catalyst in biphasic ecological and renewable n-butanol/water (1:1, 1.5:1, 2:1, and 2.5:1 ratios) as the dissolvent. For xylose conversion, an enhanced catalytic performance and the largest initial reaction rate, pseudo-first-order constant, and TOF were obtained using a butanol/water ratio of 1.5:1 as solvent. This is the first time such a high xylose conversion (100%) and 46% selectivity has been reported on the MCM-41-SO_3H catalyst in the presence of a mixture of butanol/water as a solvent medium. The catalytic production of furfural from hemicellulose on the MCM-41-SO_3H catalyst was also studied. The recycling evaluation test of the MCM-41-SO_3H catalyst indicated that the recovered catalyst needs to be submitted to a sulfonation process to reach a furfural yield closer to that of the fresh catalyst. Despite the results obtained for conversion and selectivity to furfural, the recycling of the catalyst showed that there was leaching of the –SO_3H groups from the active sites. This was mainly determined based on the presence of sulfur detected in the reaction medium, which was less than 0.03 g S. It is necessary to continue working on the optimization of the development conditions of sulfonated acid catalysts as well as the regeneration conditions in order

to use this type of material in practical applications, thus allowing the transformation of lignocellulosic raw material into value-added products.

Supplementary Materials: The following supporting information can be downloaded at: https://www.mdpi.com/article/10.3390/catal13061024/s1, Figure S1: Yield of furfural upon time at different butanol:water ratio for the non-catalytic and MCM-41 and MCM-41-SO_3H catalytic xylose conversion; Figure S2: Xylose and hemicellulose conversion for fresh and recycles MCM-41-SO_3H catalyst at a butanol:water ratio= 1.5:1; Figure S3. Furfural yield in MCM-41-SO_3H catalyzed reaction (red) and compared to furfural yield during hot filtration experiment. The reaction was stopped after 30 min, filtered while hot and continued without the presence of the catalyst (blue); Table S1: Xylose and xylan conversion to furfural in different catalysis conditions.

Author Contributions: Y.O.; methodology, C.H.; formal analysis, J.S.; software, C.S.; supervision, C.P.; writing—review and editing, G.P. writing—review and editing. All authors have read and agreed to the published version of the manuscript.

Funding: This research was funded by ANID Millennium Science Initiative Program NCN2021_090, ANID FONDECYT GRANT 1210142, and FONDECYT Postdoctoral 3210008. Yasnina Olivares would like to thank the Master Scholarship Conicyt 22201245.

Data Availability Statement: Data availability statements are available in section "MDPI Research Data Policies" at https://www.mdpi.com/ethics (accessed on 19 June 2023).

Conflicts of Interest: The authors declare no conflict of interest.

References

1. Haldar, D.; Purkait, M.K. A Review on the Environment-Friendly Emerging Techniques for Pretreatment of Lignocellulosic Biomass: Mechanistic Insight and Advancements. *Chemosphere* **2021**, *264*, 128523. [CrossRef] [PubMed]
2. Wang, F.; Ouyang, D.; Zhou, Z.; Page, S.J.; Liu, D.; Zhao, X. Lignocellulosic Biomass as Sustainable Feedstock and Materials for Power Generation and Energy Storage. *J. Energy Chem.* **2021**, *57*, 247–280. [CrossRef]
3. Sella Kapu, N.; Trajano, H.L. Review of Hemicellulose Hydrolysis in Softwoods and Bamboo. *Biofuels Bioprod. Bioref.* **2014**, *8*, 857–870. [CrossRef]
4. Yang, H.; Yi, N.; Zhao, S.; Qaseem, M.F.; Zheng, B.; Li, H.; Feng, J.X.; Wu, A. min Characterization of Hemicelluloses in Sugarcane (Saccharum Spp. Hybrids) Culm during Xylogenesis. *Int. J. Biol. Macromol.* **2020**, *165*, 1119–1128. [CrossRef] [PubMed]
5. Mariscal, R.; Maireles-Torres, P.; Ojeda, M.; Sádaba, I.; López Granados, M. Furfural: A Renewable and Versatile Platform Molecule for the Synthesis of Chemicals and Fuels. *Energy Environ. Sci.* **2016**, *9*, 1144–1189. [CrossRef]
6. Werpy, T.; Petersen, G. *Top Value Added Chemicals from Biomass Volume I—Results of Screening for Potential Candidates from Sugars and Synthesis Gas*; U.S. Department of Energy, Office of Scientific and Technical Information: Oak Ridge, TN, USA, 2004.
7. Mizuno, N.; Misono, M. Heterogeneous Catalysis. *Chem. Rev.* **1998**, *98*, 199–216. [CrossRef]
8. Sarrafi, Y.; Mehrasbi, E.; Mashalchi, S.Z. MCM-41-SO_3H: An Efficient, Reusable, Heterogeneous Catalyst for the One-Pot, Three-Component Synthesis of Pyrano[3,2-b]Pyrans. *Res. Chem. Intermed.* **2021**, *47*, 1729–1741. [CrossRef]
9. Beck, J.S.; Vartulli, J.C.; Roth, W.J.; Leonowicz, M.E.; Kresge, C.T.; Schmitt, K.D.; Chu, C.T.-W.; Olson, D.H.; Sheppard, E.W.; McCullen, S.B.; et al. A New Family of Mesoporous Molecular Sieves Prepared with Liquid Crystal Templates. *J. Am. Chem. Soc.* **1992**, *114*, 10834–10843. [CrossRef]
10. Brezoiu, A.M.; Deaconu, M.; Nicu, I.; Vasile, E.; Mitran, R.A.; Matei, C.; Berger, D. Heteroatom Modified MCM-41-Silica Carriers for Lomefloxacin Delivery Systems. *Microporous Mesoporous Mater.* **2019**, *275*, 214–222. [CrossRef]
11. Meynen, V.; Cool, P.; Vansant, E.F. Verified Syntheses of Mesoporous Materials. *Microporous Mesoporous Mater.* **2009**, *125*, 170–223. [CrossRef]
12. Kresge, C.T.; Leonowiccz, M.E.; Roth, W.J.; Vartuli, J.C.; Beck, J.S. Ordered Mesoporous Molecular Sieves Synthesized by a Liquid-Crystal Template Mechanism. *Nature* **1992**, *359*, 710–712. [CrossRef]
13. Safaei, S.; Mohammadpoor-Baltork, I.; Khosropour, A.R.; Moghadam, M.; Tangestaninejad, S.; Mirkhani, V. SO_3H-Functionalized MCM-41 as an Efficient Catalyst for the Combinatorial Synthesis of 1H-Pyrazolo-[3,4-b]Pyridines and Spiro-Pyrazolo-[3,4-b]Pyridines. *J. Iran. Chem. Soc.* **2017**, *14*, 1583–1589. [CrossRef]
14. Jeong, G.H.; Kim, E.G.; Kim, S.B.; Park, E.D.; Kim, S.W. Fabrication of Sulfonic Acid Modified Mesoporous Silica Shells and Their Catalytic Performance with Dehydration Reaction of D-Xylose into Furfural. *Microporous Mesoporous Mater.* **2011**, *144*, 134–139. [CrossRef]
15. Shi, X.; Wu, Y.; Yi, H.; Rui, G.; Li, P.; Yang, M.; Wang, G. Selective Preparation of Furfural from Xylose over Sulfonic Acid Functionalized Mesoporous Sba-15 Materials. *Energies* **2011**, *4*, 669–684. [CrossRef]
16. Dias, A.S.; Pillinger, M.; Valente, A.A. Dehydration of Xylose into Furfural over Micro-Mesoporous Sulfonic Acid Catalysts. *J. Catal.* **2005**, *229*, 414–423. [CrossRef]

17. Zhang, J.; Zhuang, J.; Lin, L.; Liu, S.; Zhang, Z. Conversion of D-Xylose into Furfural with Mesoporous Molecular Sieve MCM-41 as Catalyst and Butanol as the Extraction Phase. *Biomass Bioenergy* **2012**, *39*, 73–77. [CrossRef]
18. Bozell, J.J.; Petersen, G.R. Technology Development for the Production of Biobased Products from Biorefinery Carbohydrates—The US Department of Energy's "Top 10" Revisited. *Green Chem.* **2010**, *12*, 539–554. [CrossRef]
19. Lima, S.; Pillinger, M.; Valente, A.A. Dehydration of D-Xylose into Furfural Catalysed by Solid Acids Derived from the Layered Zeolite Nu-6(1). *Catal. Commun.* **2008**, *9*, 2144–2148. [CrossRef]
20. Lima, S.; Neves, P.; Antunes, M.M.; Pillinger, M.; Ignatyev, N.; Valente, A.A. Conversion of Mono/Di/Polysaccharides into Furan Compounds Using 1-Alkyl-3-Methylimidazolium Ionic Liquids. *Appl. Catal. A Gen.* **2009**, *363*, 93–99. [CrossRef]
21. Serrano-Ruiz, J.C.; Campelo, J.M.; Francavilla, M.; Romero, A.A.; Luque, R.; Menéndez-Vázquez, C.; García, A.B.; García-Suárez, E.J. Efficient Microwave-Assisted Production of Furfural from C5 Sugars in Aqueous Media Catalysed by Brönsted Acidic Ionic Liquids. *Catal. Sci. Technol.* **2012**, *2*, 1828–1832. [CrossRef]
22. Marin-astorga, N.; Pecchi, G.; Reyes, P. Ordered Mesoporous Silicates Of Mcm-41 Type As Supports Of Pt Catalysts For The Enantioselective Hydrogenation Of 1-Phenyl-1, 2-Propanedione. *React. Kinet. Catal. Lett.* **2006**, *87*, 121–128. [CrossRef]
23. Rostamizadeh, S.; Amani, A.M.; Mahdavinia, G.H.; Amiri, G.; Sepehrian, H. Ultrasound Promoted Rapid and Green Synthesis of 1,8-Dioxo-Octahydroxanthenes Derivatives Using Nanosized MCM-41-SO_3H as a Nanoreactor, Nanocatalyst in Aqueous Media. *Ultrason. Sonochem.* **2010**, *17*, 306–309. [CrossRef] [PubMed]
24. Khan, A.L.; Klaysom, C.; Gahlaut, A.; Li, X.; Vankelecom, I.F.J. SPEEK and Functionalized Mesoporous MCM-41 Mixed Matrix Membranes for CO 2 Separations. *J. Mater. Chem.* **2012**, *22*, 20057–20064. [CrossRef]
25. Wang, S.; Shi, Y.; Ma, X. Microwave Synthesis, Characterization and Transesterification Activities of Ti-MCM-41. *Microporous Mesoporous Mater.* **2012**, *156*, 22–28. [CrossRef]
26. Hermida, L.; Zuhairi Abdullah, A.; Rahman Mohamed, A. Synthesis of Monoglyceride through Glycerol Esterification with Lauric Acid over Propyl Sulfonic Acid Post-Synthesis Functionalized SBA-15 Mesoporous Catalyst. *Chem. Eng. J.* **2011**, *174*, 668–676. [CrossRef]
27. Sreevardhan Reddy, S.; David Raju, B.; Siva Kumar, V.; Padmasri, A.H.; Narayanan, S.; Rama Rao, K.S. Sulfonic Acid Functionalized Mesoporous SBA-15 for Selective Synthesis of 4-Phenyl-1,3-Dioxane. *Catal. Commun.* **2007**, *8*, 261–266. [CrossRef]
28. Sheng, X.; Gao, J.; Han, L.; Jia, Y.; Sheng, W. One-Pot Synthesis of Tryptophols with Mesoporous MCM-41 Silica Catalyst Functionalized with Sulfonic Acid Groups. *Microporous Mesoporous Mater.* **2011**, *143*, 73–77. [CrossRef]
29. Kaiprommarat, S.; Kongparakul, S.; Reubroycharoen, P.; Guan, G.; Samart, C. Highly Efficient Sulfonic MCM-41 Catalyst for Furfural Production: Furan-Based Biofuel Agent. *Fuel* **2016**, *174*, 189–196. [CrossRef]
30. Karnjanakom, S.; Kongparakul, S.; Chaiya, C.; Reubroycharoen, P.; Guan, G.; Samart, C. Biodiesel Production from Hevea Brasiliensis Oil Using SO_3H-MCM-41 Catalyst. *J. Environ. Chem. Eng.* **2016**, *4*, 47–55. [CrossRef]
31. Bukallah, S.B.; Bumajdad, A.; Khalil, K.M.S.; Zaki, M.I. Characterization of Mesoporous VOx/MCM-41 Composite Materials Obtained via Post-Synthesis Impregnation. *Appl. Surf. Sci.* **2010**, *256*, 6179–6185. [CrossRef]
32. Rathod, P.V.; Mujmule, R.B.; Chung, W.-J.; Jadhav, A.R.; Kim, H. Efficient Dehydration of Glucose, Sucrose, and Fructose to 5-Hydroxymethylfurfural Using Tri-Cationic Ionic Liquids. *Catal. Lett.* **2019**, *149*, 672–687. [CrossRef]
33. Chen, K.; Yan, X.; Li, J.; Jiao, T.; Cai, C.; Zou, G.; Wang, R.; Wang, M.; Zhang, L.; Peng, Q. Preparation of Self-Assembled Composite Films Constructed by Chemically-Modified MXene and Dyes with Surface-Enhanced Raman Scattering Characterization. *Nanomaterials* **2019**, *2*, 284. [CrossRef]
34. Hino, M.; Kurashige, M.; Matsuhashi, H.; Arata, K. The Surface Structure of Sulfated Zirconia: Studies of XPS and Thermal Analysis. *Thermochim. Acta* **2006**, *441*, 35–41. [CrossRef]
35. Herrera, C.; Fuentealba, D.; Ghampson, I.T.; Sepulveda, C.; García-Fierro, J.L.; Canales, R.I.; Escalona, N. Selective Conversion of Biomass-Derived Furfural to Cyclopentanone over Carbon Nanotube-Supported Ni Catalyst in Pickering Emulsions. *Catal. Commun.* **2020**, *144*. [CrossRef]
36. Moreau, C.; Durand, R.; Peyron, D.; Duhamet, J.; Rivalier, P. Selective Preparation of Furfural from Xylose over Microporous Solid Acid Catalysts. *Ind. Crops Prod.* **1998**, *7*, 95–99. [CrossRef]
37. Rivalier, P.; Duhamet, J.; Moreau, C.; Durand, R. Development of a Continuous Catalytic Heterogeneous Column Reactor with Simultaneous Extraction of an Intermediate Product by an Organic Solvent Circulating in Countercurrent Manner with the Aqueous Phase. *Catal. Today* **1995**, *24*, 165–171. [CrossRef]
38. Karimi, B.; Zareyee, D. Design of a Highly Efficient And-Tolerant Sulfonic Acid Based on Tunable Ordered Silica for the von Pechmann Reacton. *Org. Lett.* **2008**, *10*, 3989–3992. [CrossRef]
39. Liu, C.; Wei, L.; Yin, X.; Wei, M.; Xu, J.; Jiang, J.; Wang, K. Selective Conversion of Hemicellulose into Furfural over Low-Cost Metal Salts in a γ-Valerolactone/Water Solution. *Ind. Crops Prod.* **2020**, *147*, 112248. [CrossRef]
40. Agirrezabal-Telleria, I.; Gandarias, I.; Arias, P.L. Heterogeneous Acid-Catalysts for the Production of Furan-Derived Compounds (Furfural and Hydroxymethylfurfural) from Renewable Carbohydrates: A Review. *Catal. Today* **2014**, *234*, 42–58. [CrossRef]

41. Madon, R.J.; Boudart, M. Experimental Criterion for the Absence of Artifacts in the Measurement of Rates of Heterogeneous Catalytic Reactions. *Ind. Eng. Chem. Fundam.* **1982**, *21*, 438–447. [CrossRef]
42. Troncoso-Ortega, E.; Castillo, R.D.P.; Reyes-Contreras, P.; Castaño-Rivera, P.; Teixeira Mendonça, R.; Schiappacasse, N.; Parra, C. Effects on Lignin Redistribution in Eucalyptus Globulus Fibres Pre-Treated by Steam Explosion: A Microscale Study to Cellulose Accessibility. *Biomolecules* **2021**, *11*, 507. [CrossRef] [PubMed]